

*Correspondence: Asmat Ullah
+33 (0) 7 58 74 93 09
asmat.ullah12@hotmail.com

Extremes in South African Rainfall: Mean Characteristics and Seamless Variability Across Multiple Timescales

May 25, 2022

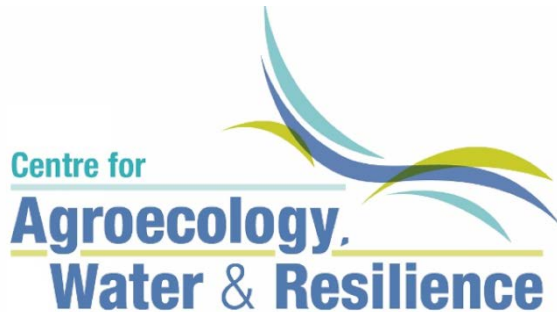


Asmat Ullah^{1*} ; Benjamin Pohl¹ ; Julien Pergaud¹ ; Bastien Dieppois² ; Mathieu Rouault³

¹ Centre de Recherches de Climatologie, UMR 6282 Biogéosciences, CNRS/ Université de Bourgogne Franche-Comté, Dijon, France

² Centre for Agroecology, Water and Resilience, Coventry University, Coventry, UK

³ Nansen Tutu Center for Marine Environmental Research, Department of Oceanography, University of Cape Town, South Africa

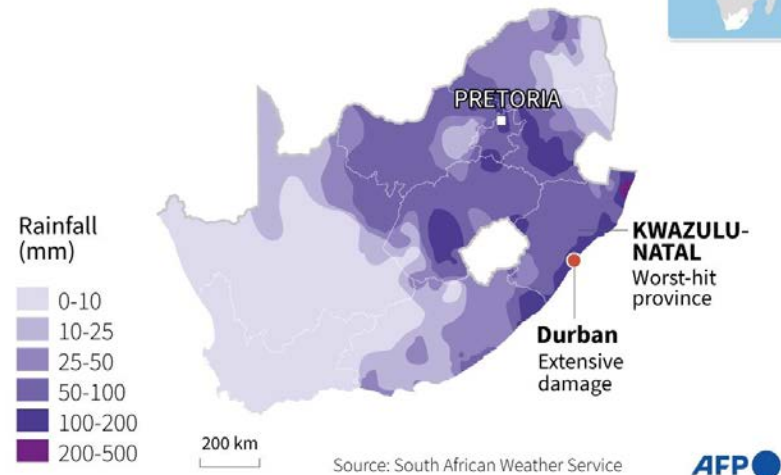


Motivation: A recent heavy rainfall event in South Africa (8 – 12 April 2022)



Floods in South Africa

Rainfall for April 1-10, based on preliminary data



In a 24-hour period spanning 11–12 April, Virginia Airport recorded 304 mm (12.0 in) of Rainfall

Death toll = 443 (65 still missing)

Economic losses = \$5.7 billion (early estimate)

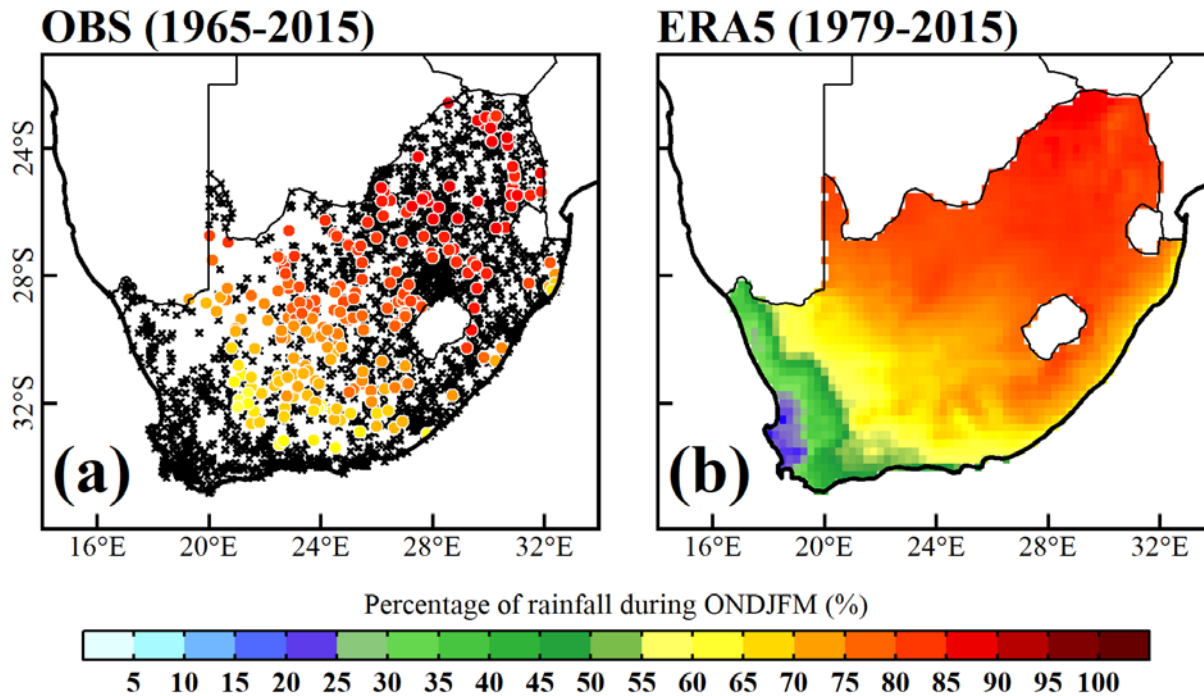
Households affected = 13,500

It is one of the deadliest natural disasters in the country in the 21st century after 1987 floods

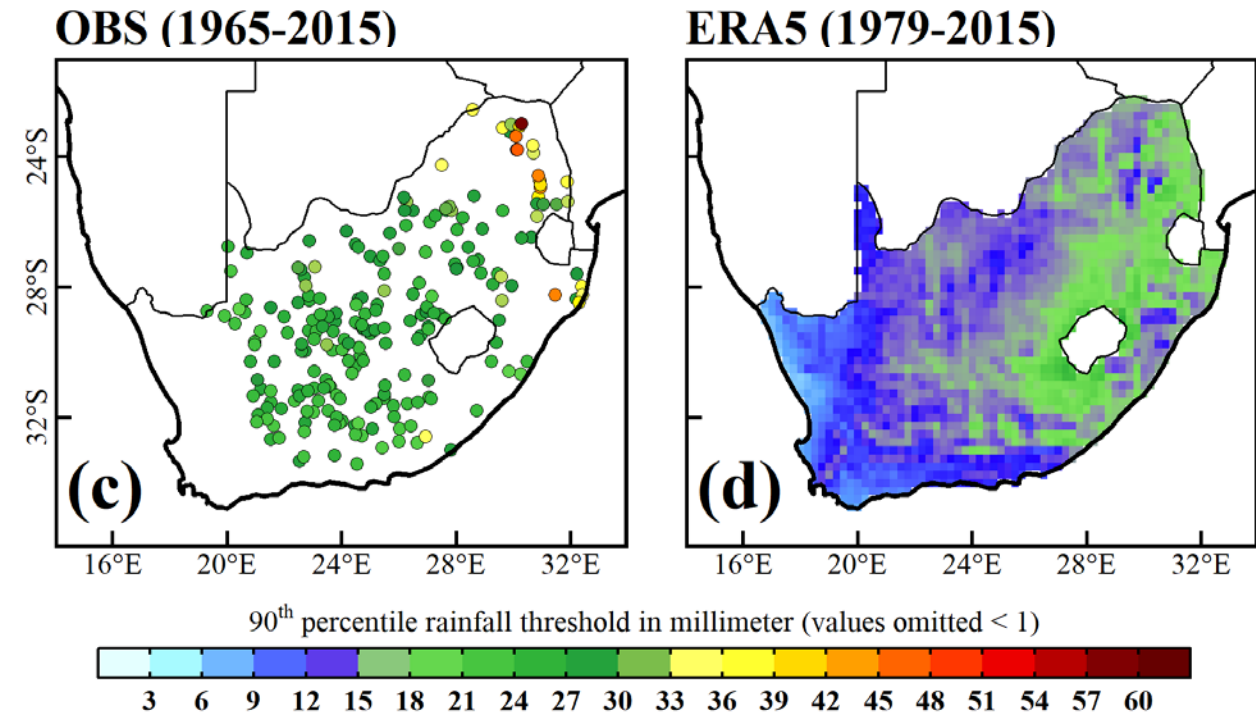


Study area and Methods

Seasonality test



Local 90th Percentile threshold

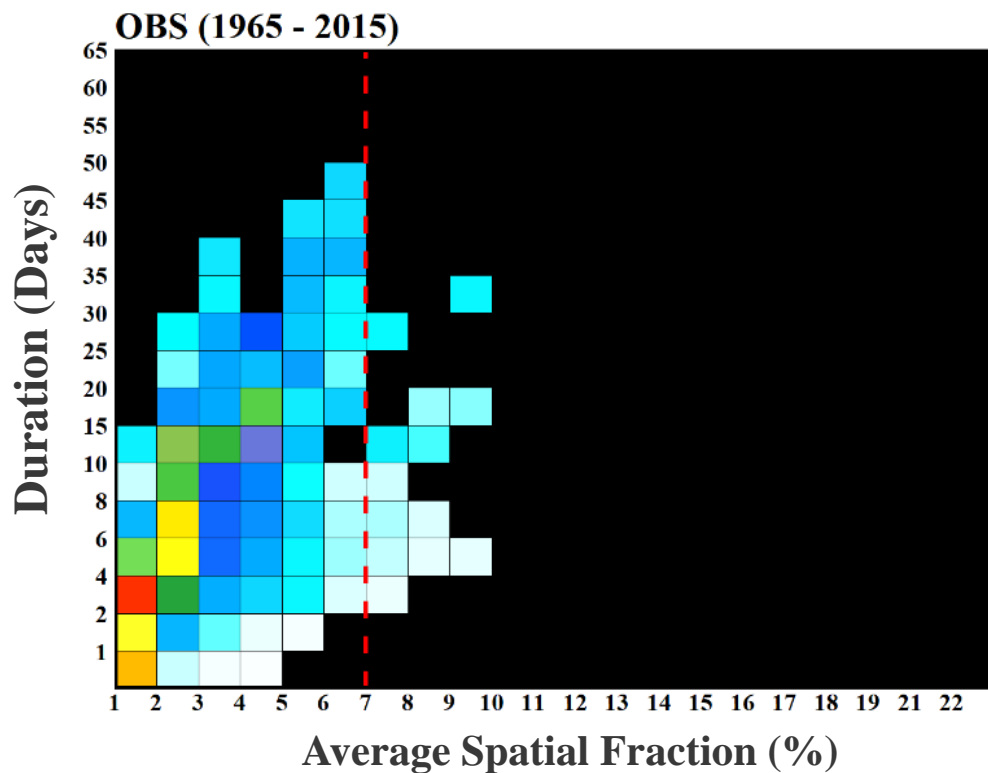


- To calculate 90th Percentile (ONDJFM: 1965-2015) for OBS and 1979-2015 for ERA5
- Longer period and extended season ensures robustness of local threshold
- Overall study period: Austral Summer Season (NDJF: 1979-2015)

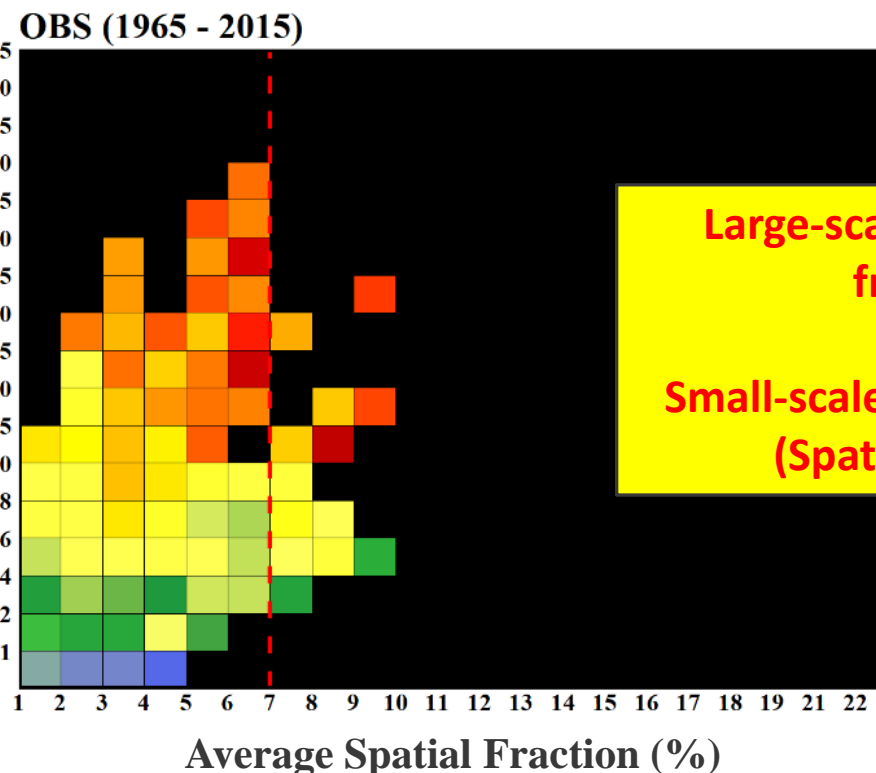


Results: Typology of rainfall extremes

a) Frequency



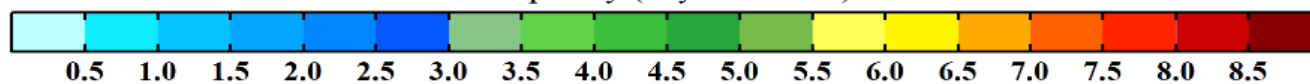
b) Intensity



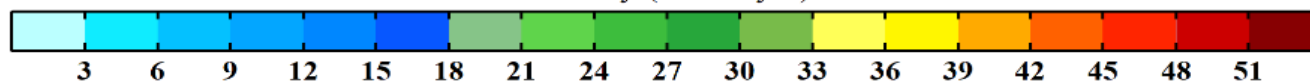
Large-scale extremes (Spatial fraction $\geq 7\%$)

Small-scale or localized extremes (Spatial fraction $< 7\%$)

Frequency (days.season⁻¹)

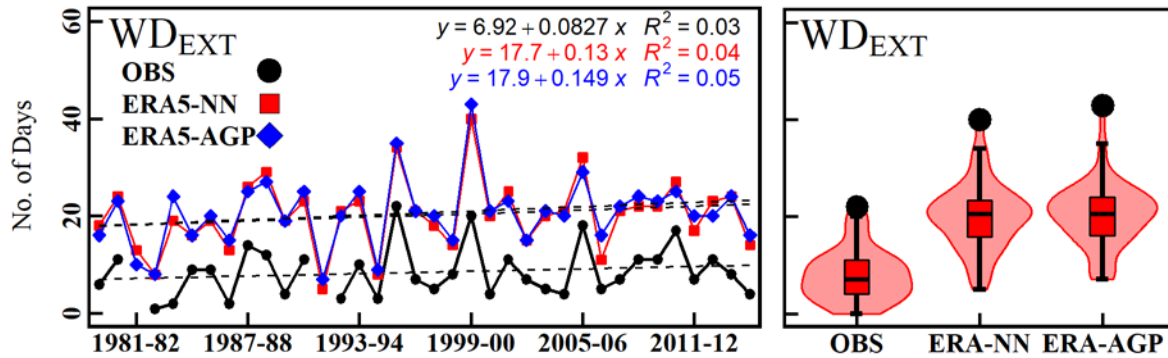


Intensity (mm.day⁻¹)

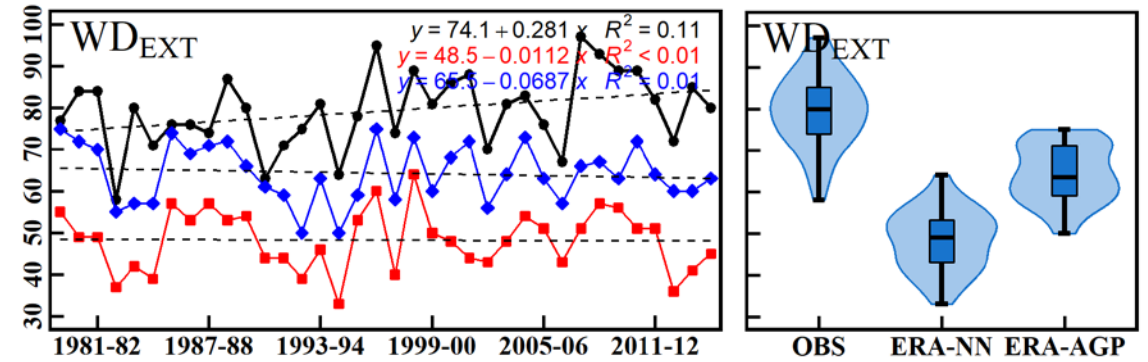


Results (Mean characteristics)

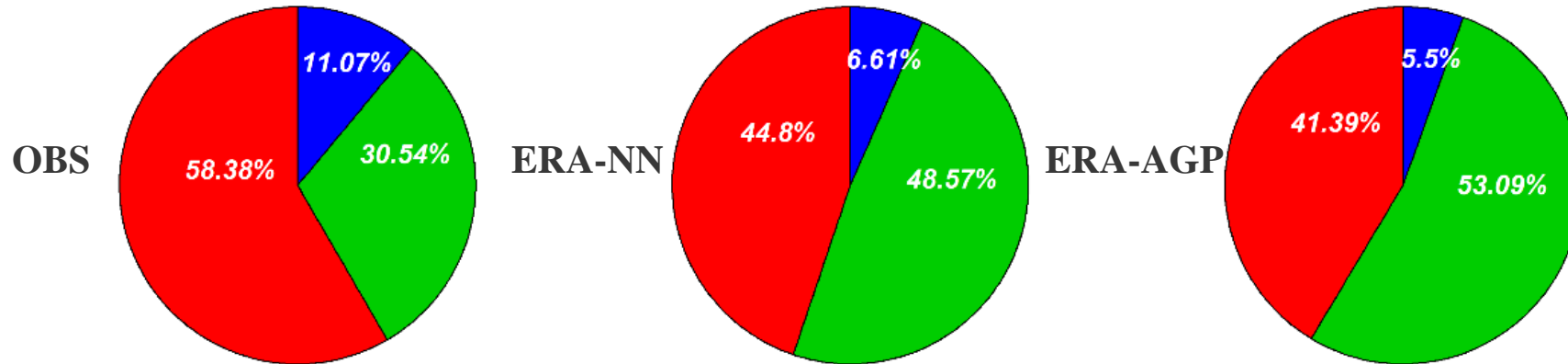
a) ISDs (Large-scale Extremes)



b) ISDs (Small-scale Extremes)

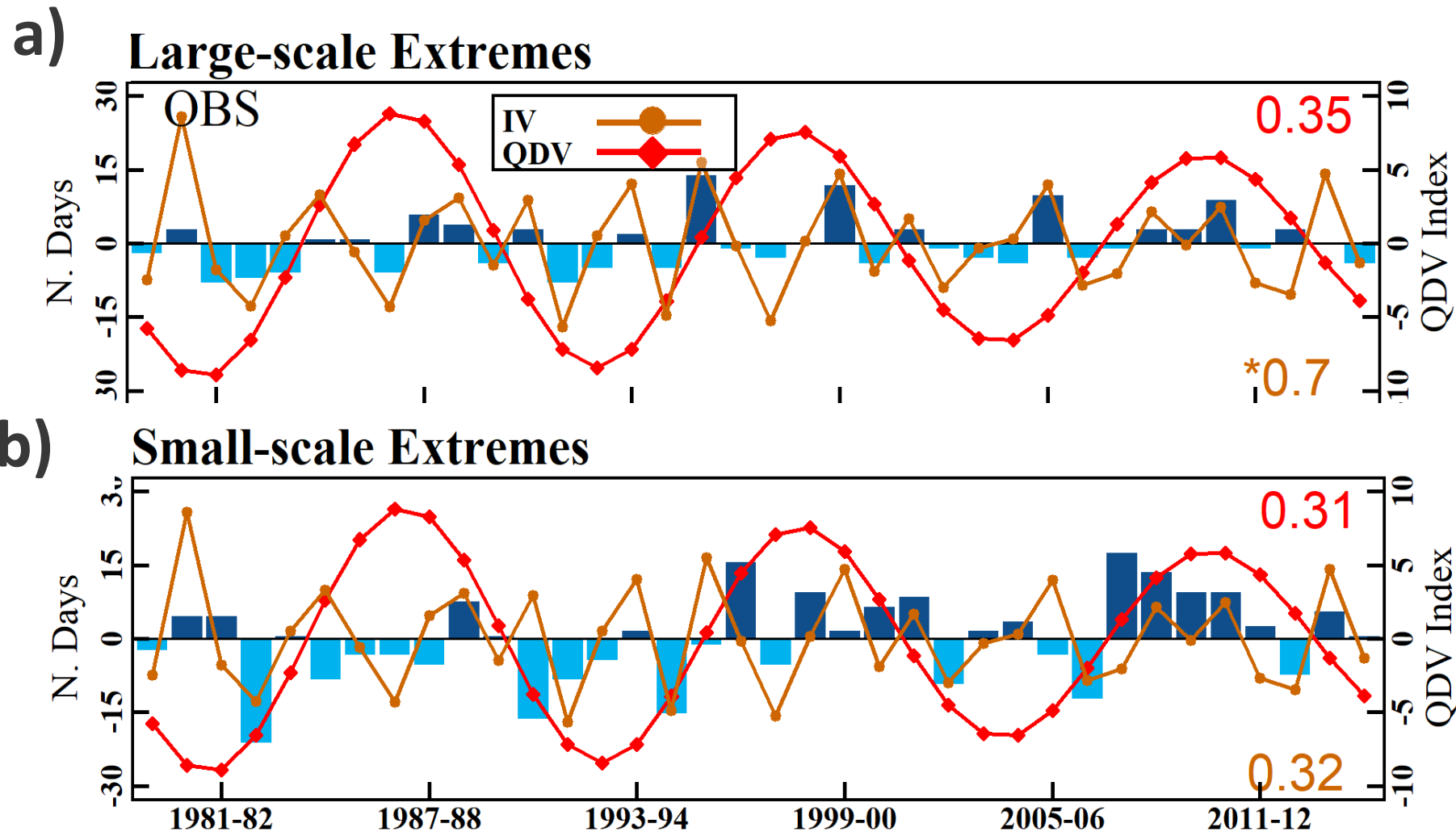


c) Contribution of rainfall during austral summer season (NDJF)



Large-Scale Small-Scale Non-Extreme

Results: Variability of extremes at low frequency timescales (ENSO and IPO)



The time series of Summer Rainfall Index (SRI) filtered at 2–8 year interannual (IV) and 8–13 year's quasi decadal timescales (QDV) using a *Fast Fourier Transform* filtering (Dieppo et al 2016). The filtered SRI displays different periodicities, where IV and QDV were found to be primarily associated with ENSO and the Interdecadal Pacific Oscillation, respectively.



Risk assessment at low-frequency timescales

Risk Ratio RR is defined as the ratio of the probability of an ISD under a factual scenario (P_F), to that probability under a counterfactual scenario (P_{CF}) (cf. Paciorek *et al.*, 2018) and is given by the following equation:

$$RR = \frac{P_F}{P_{CF}} = \frac{\left[\frac{a}{(a+b)} \right]_{IV | QDV}}{\left[\frac{x}{(x+y)} \right]_{IV | QDV}}$$

where a (b) is the sum of a given ISD (i.e., number of wet days or total rainfall) when it lies in its positive (negative) phase of anomaly, simultaneously when IV or QDV is in the positive phase of the anomaly, representing PF scenario. Similarly, x (y) is the sum of a given ISD (i.e., number of wet days or total rainfall) when it lies in its positive (negative) phase of anomaly, simultaneously when the IV or QDV is in the negative phase of the anomaly, representing PCF scenario.

RR is computed at normal and Strong opposite phases of SRI (± 0.5 SD)



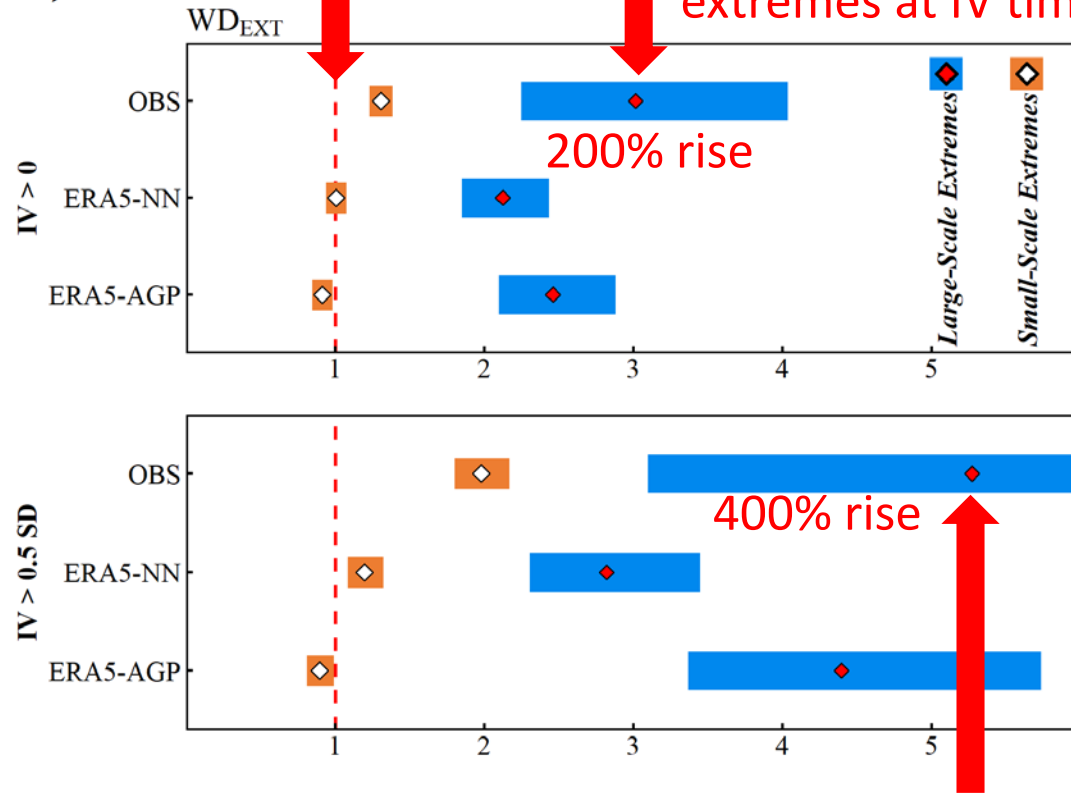
Cont...



a) IV

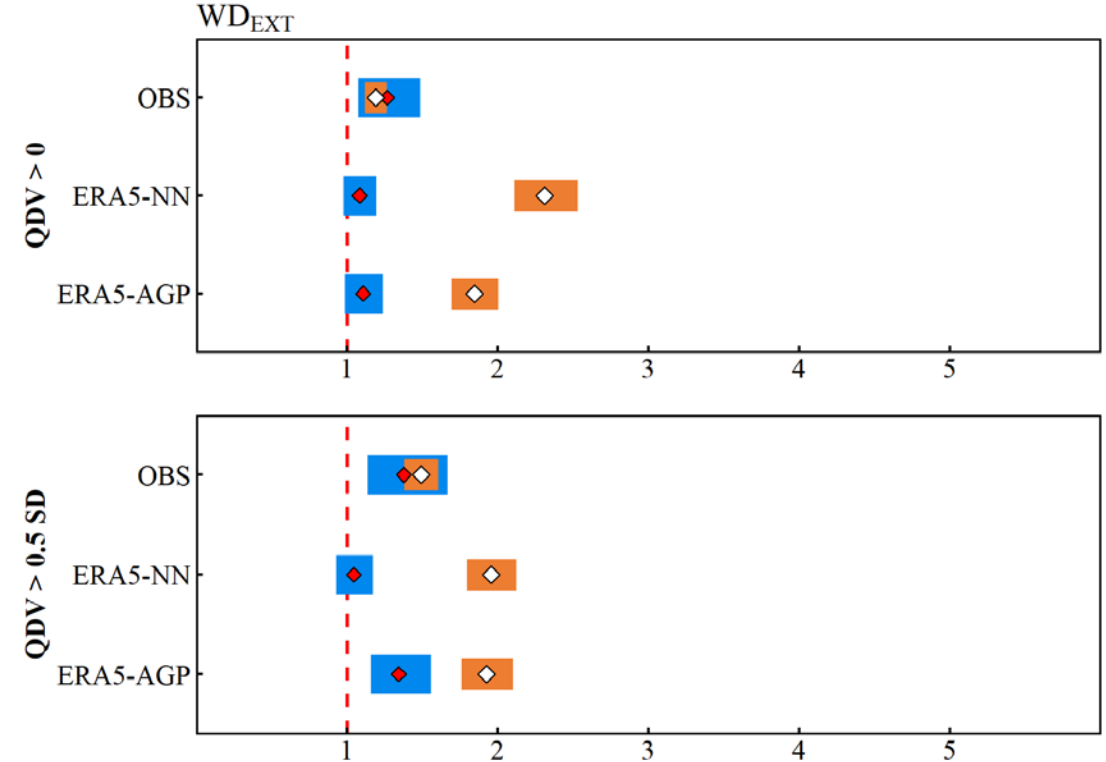
No risk

High risk of Large-scale extremes at IV timescale



Extremely high risk of Large-scale extremes at IV timescale

b) QDV



Moderate risk of extremes at QDV timescale either at normal or >0.5 SD

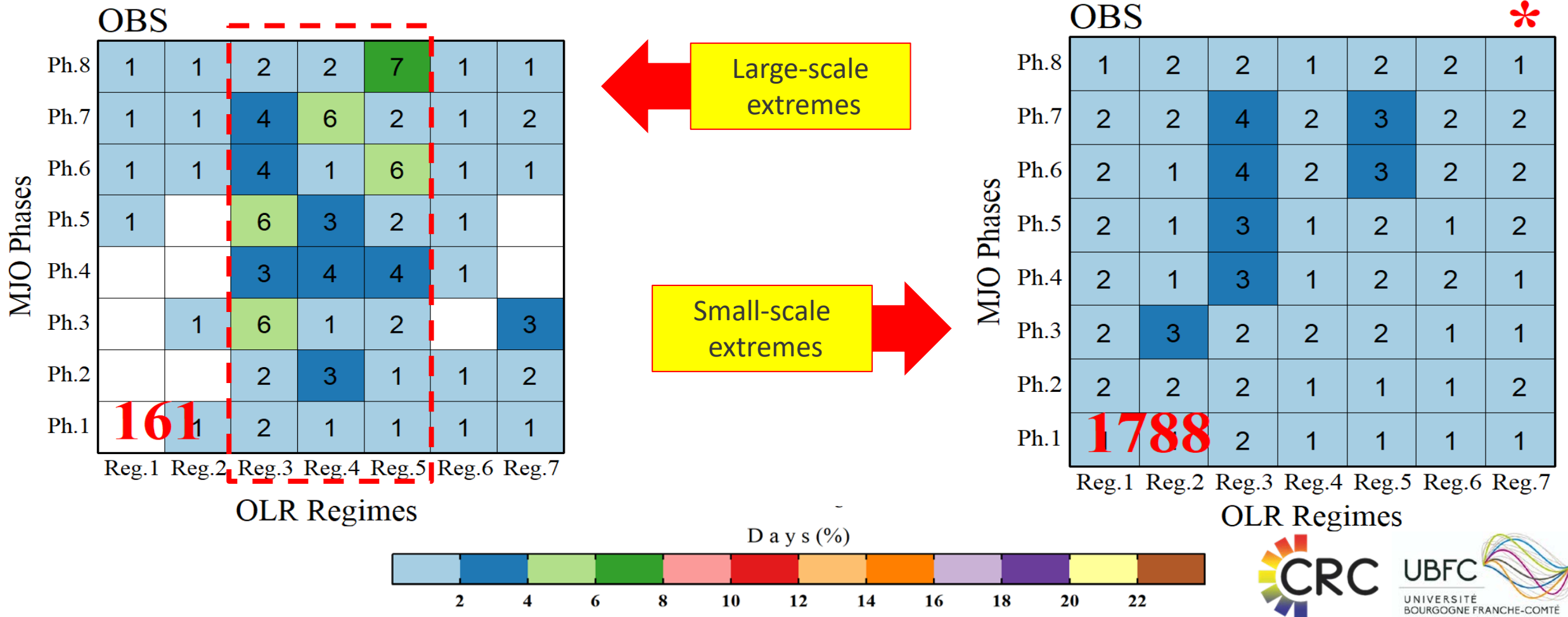
Plain language summary!

For instance, observed data show an average of 8 days.season⁻¹ associated with large-scale extremes, but the risk of such extreme wet days can exceed 24 days when IV in its strong positive phase, which tends to coincide to strong La Niña events.

Results: Variability of extremes at high-frequency timescales (Frequency)



At high-frequencies, extremes are associated with synoptic-scale variability related to seven convective regimes of Tropical Temperate Troughs (TTTs: 3–7 days; Fauchareau et al. 2009) and eight phases related to intraseasonal variability of the Madden-Julien Oscillation (MJO: 30–60 days; Wheeler and Hendon 2004).



Risk assessment at high-frequency timescales

$$RR = \frac{P_F}{P_{CF}} = \frac{\left[\frac{a}{(a+b)} \right]_{\text{Regime and Phase of interest}}}{\left[\frac{x}{(x+y)} \right]_{\text{Regime and Phase of interest}}}$$

where a (b) is the sum of extreme (non-extreme) days when MJO > 1.
Similarly, the x (y) is the sum of extreme (non-extreme) days when MJO < 1.

Risk of Large-scale
extremes suppressed

MJO Phases 1-2

Dry-Phases

Large-Scale Extremes

MJO Phases 3-5

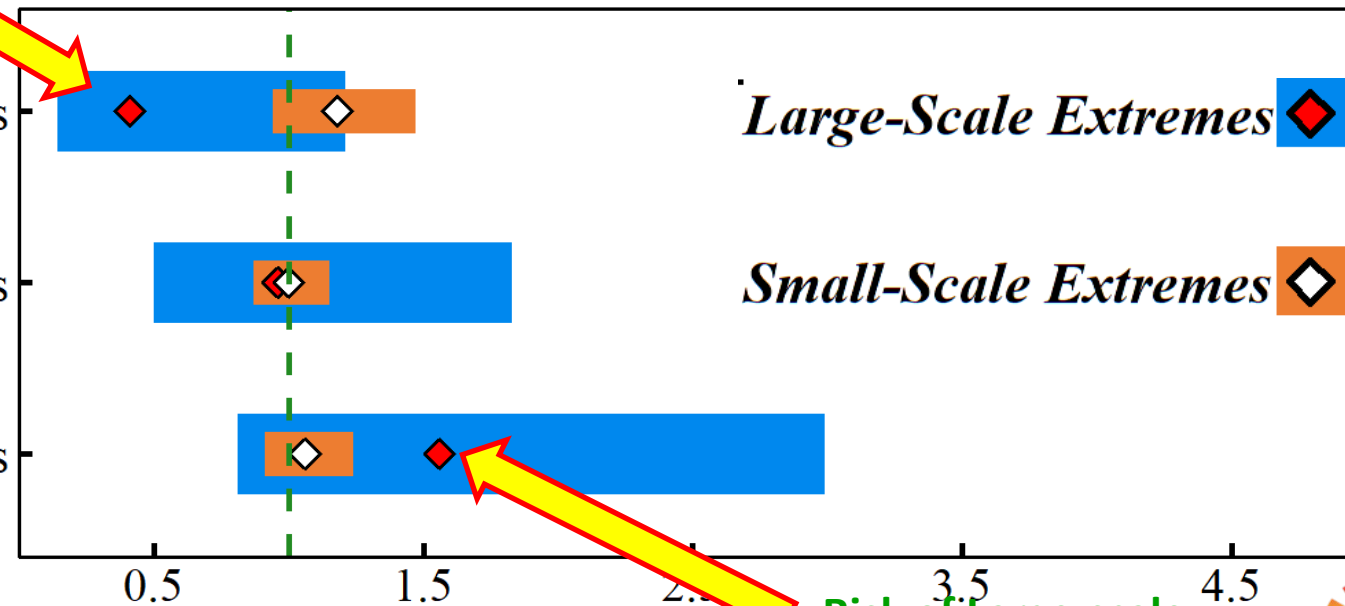
Moderate-Phases

Small-Scale Extremes

MJO Phases 6-8

Wet-Phases

Regime 5



Risk of Large-scale
extremes enhanced



Summary and Conclusions

- The results demonstrate that using 7% of spatial fraction simultaneously exceeding the local threshold of the 90th percentile produces remarkable results in characterizing rainfall extremes into large- and small-scale extremes.
- Austral summer total rainfall is found to be primarily shaped by large-scale extremes.
- We also find that during small-scale events the extreme conditions are found sporadic over the region contrasting with large-scale events for which extreme conditions are found over a larger and coherent region.
- At the low-frequency timescale, the frequency of large-scale extremes strongly varies when IV timescale lies in positive phase while modulation in total rainfall associated with large-scale extremes are mainly related to the QDV timescale.
- At the high-frequency timescale, the synoptic-scale variability associated with TTT events is related to large-scale extremes as nearly 75% of such events occurring during regimes 3 to 5 whereas small-scale extremes are found equiprobable during all TTT synoptic regimes.
- The probability of large-scale extremes in TTT regime 5 is significantly enhanced during MJO phases 6 to 8 while it is suppressed during phases 1 to 2.



References

- Dieppois B, Pohl B, Rouault M, New M, Lawler D, Keenlyside N. 2016. Interannual to interdecadal variability of winter and summer southern African rainfall, and their teleconnections. *Journal of Geophysical Research*. <https://doi.org/10.1002/2015JD024576>.
- Fauchereau N, Pohl B, Reason CJC, Rouault M, Richard Y. 2009. Recurrent daily OLR patterns in the Southern Africa/Southwest Indian ocean region, implications for South African rainfall and teleconnections. *Climate Dynamics*, 32(4): 575–591. <https://doi.org/10.1007/s00382-008-0426-2>.
- Paciorek CJ, Stone DA, Wehner MF. 2018. Quantifying statistical uncertainty in the attribution of human influence on severe weather. *Weather and Climate Extremes*, 20(June 2017): 69–80. <https://doi.org/10.1016/j.wace.2018.01.002>.
- Wheeler MC, Hendon HH. 2004. An all-season real-time multivariate MJO index: Development of an index for monitoring and prediction. *Monthly Weather Review*, 132(8): 1917–1932. [https://doi.org/10.1175/1520-0493\(2004\)132<1917:AARMMI>2.0.CO;2](https://doi.org/10.1175/1520-0493(2004)132<1917:AARMMI>2.0.CO;2).



Consume less to save the planet !!!

Thank you so much for your attention



Extremes in South African Rainfall:

Mean Characteristics and Seamless Variability Across Multiple Timescales

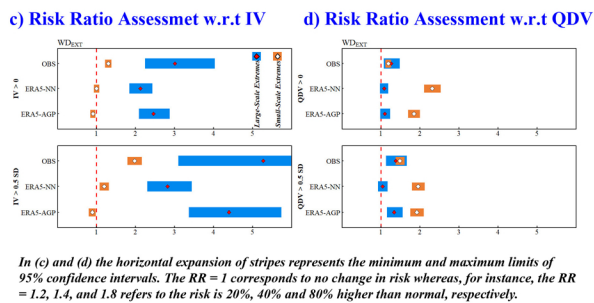
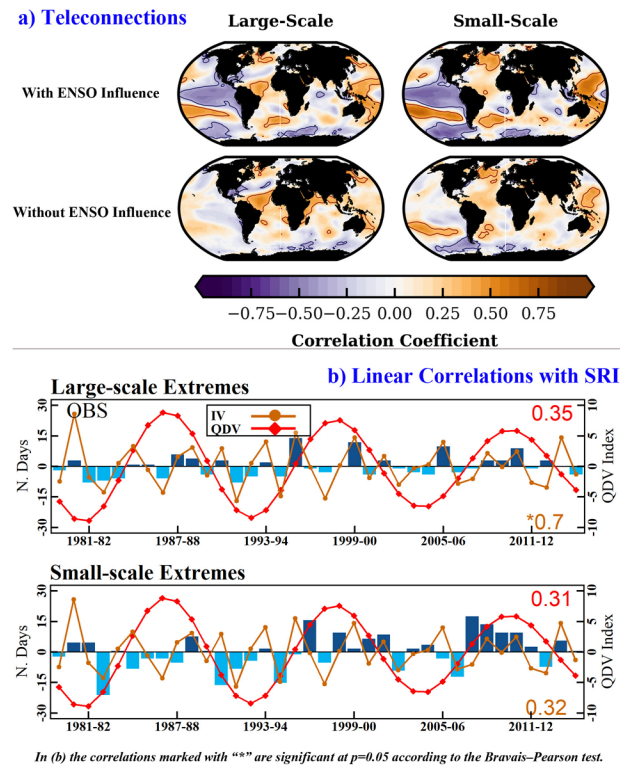
Asmat Ullah(1), Benjamin Pohl(1), Julien Pergaud(1), Bastien Dieppois(2), and Mathieu Rouault(3)

1Centre de Recherches de Climatologie, UMR 6282 Biogéosciences, CNRS/ Université de Bourgogne, Dijon, France

2Centre for Agroecology, Water and Resilience, Coventry University, Coventry, United Kingdom

3Nansen Tutu Center for Marine Environmental Research, Department of Oceanography, University of Cape Town, South Africa

1. Variability of rainfall extremes at low-frequency timescales



2. Variability of rainfall extremes at high-frequency timescales

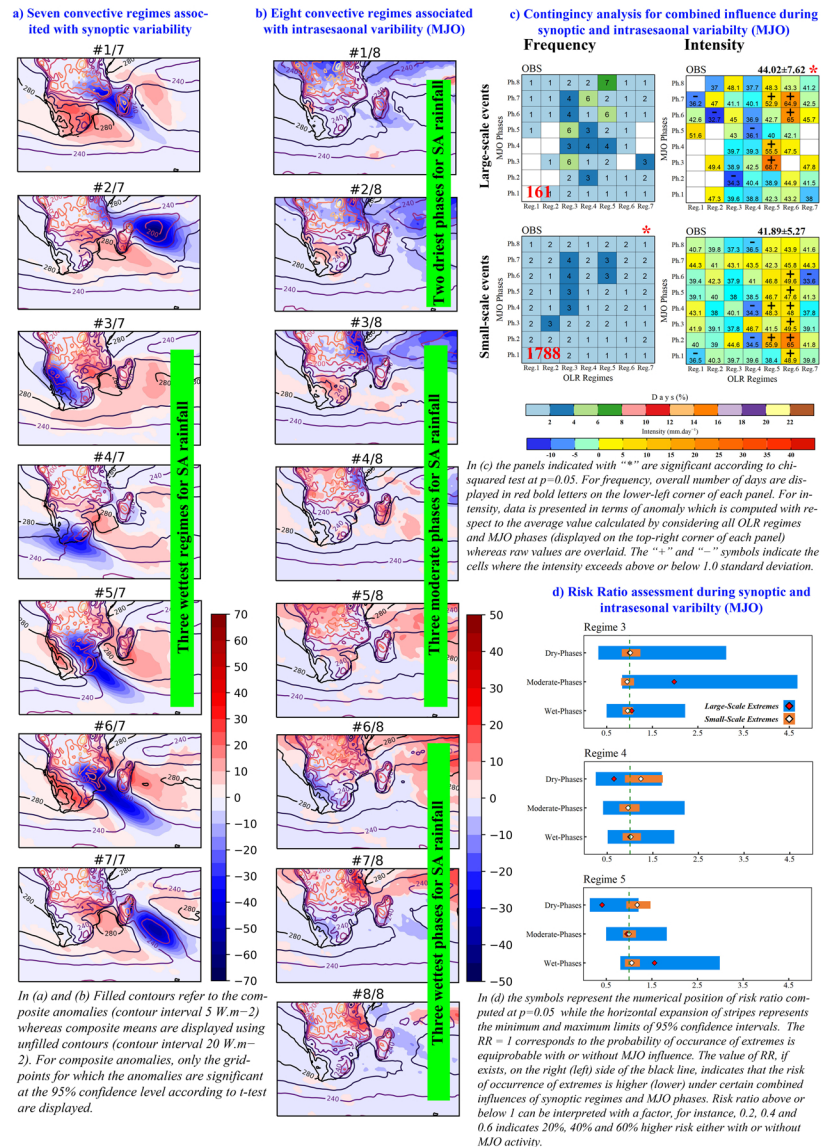


Figure 1. The correlation to global SST fields with the frequency of large- and small-scale extreme in the austral summer (a). The set of two panels in top row (bottom row) refers to the correlation to global SST with (without) ENSO influence. Anomalies of ISDs (blue bars), SRI at IV timescale (brown line) and SRI at QDV timescale (red line) are presented for wet days associated with large- and small-scale extremes (b). Estimated risk ratio computed for wet days associated with large-scale (blue stripes with red symbols) and small-scale extremes (brown stripes with white symbols) with respect to IV (c) and with respect to QDV (d) using OBS, ERA5–NN and ERA5–AGP. First row panels correspond to the RR computed by considering normal phases of IV and QDV. Second row panels correspond to the RR computed by considering strong phases of IV and QDV (i.e. ± 0.5 standard deviation).

Figure 2. Mean daily OLR anomalies illustrating seven convective regimes associated with TTTs (a) and eight phases of the MJO (b) during austral summer season (NDJF) over the period 1979–2015. Concomitance between OLR regimes and MJO phases for the frequency (left panels) and intensity (right panels) during austral summer season (NDJF) over the period 1979–2015, distributed row-wise for large-scale events and for small-scale events (c). For 8 phases of the MJO, only those days were considered where the amplitude exceeded 1 RMM. Estimated risk ratio computed for OBS by considering active and inactive days of the MJO explicitly for regime 3, 4 and 5 by considering dry (1–2), moderate (3–5), and wet (6–8), phases of the MJO (d).

Correspondence: Asmat Ullah
Email: asmat.ullah12@hotmail.com

